Vol. 86 No. 3 pp. 640–652 ACTA GEOLOGICA SINICA (English Edition) June 2012

Geophysical–Geological Interpretation and Deep-Seated Gold Deposit Prospecting in Sanshandong–Jiaojia Area, Eastern Shandong Province, China

SONG Mingchun[1, *], WAN Guopu[2], CAO Chunguo[2] and HE Chunyan[2]

1 *Shandong Provincial Bureau of Geology and Mineral Resources, Jinan 250013, China*
2 *Shandong Institute of Geophysical and Geochemical Exploration, Jinan 250013, China*

Abstract: Integrated gravitational, electrical-magnetic surveys and data processing carried out in the Sanshandao–Jiaojia area, Eastern Shandong Province, northeast China, aim to illuminate the geological characteristics of this shallow-covered area and delineate deep-seated gold prospecting targets. In this region, altogether 12 faults exert critical control on distribution of three types of Early Precambrian metamorphic rock series, i.e. those in the metamorphic rock area, in the granitic rock area underlying the metamorphic rock, and in the remnant metamorphic rock area in granites, respectively. Additionally, the faults have major effects on distribution of four Mesozoic Linglong rock bodies of granite, i.e. the Cangshang, Liangguo, Zhuqiao-Miaojia and Jincheng granites. The Sanshandao and Jiaojia Faults are two well-known regional ore-controlling faults; they have opposite dip direction, and intersect at a depth of 4500 m. Fracture alteration zones have striking geophysical differences relative to the surrounding county rocks. The two faults extend down along dip direction in a gentle wave form, and appear at some steps with different dips. These steps comprise favorable gold prospecting areas, consistent with a step metallogenic model. Six deep-seated gold-prospecting targets are delineated, i.e. Jincheng-Qianchenjia, Xiaoxizhuang-Zhaoxian, Xiyou-Wujiazhuangzi, Xiangyangling-Xinlicun, Panjiawuzi and Miaojia-Pinglidian.

Key words: geophysical interpretation, deep-seated gold deposit, prospecting and prediction, tectonic control, Shandong Province

1 Introduction

Eastern Shandong Province is an important gold concentration area in China. Geophysical prospecting methods exert a key effect on gold prospecting in this region (Zhou, 1989; Jiang et al., 1997; Niu and Luo, 1995; Gu et al., 1996; Yang et al., 2000; He et al., 2005; Li et al., 2007). Some shallow covered gold deposits in the northwestern part of Eastern Shandong Province have been discovered with geophysical methods, of which the Cangshang gold deposit in Laizhou city is a typical one discovered using both geological and geophysical methods (Li et al., 2007).

Since 2005, prospecting of deep-seated gold deposits in Eastern Shandong Province has achieved marked success. Many large and super-large deep-seated gold deposits, such as those in Sizhuang, Matang and Jiaojia (Song et al., 2007, 2008, 2010a, 2010b) and in the Sanshandao ore field were discovered. Till now, proven and being explored resources have reached 1000 t, equivalent to those previously discovered shallower than 500 m. Geophysical methods have been widely applied to the deep-seated gold search in the region (Niu et al., 2004). In this contribution, we offer a geological-geophysical metallogenic model and prospecting prediction, based on previous deep prospecting results in the Sanshandao–Jiaojia area.

2 Regional Geology

In the Sanshandao-Jiaojia area, bedrock comprises mainly Mesozoic granites and Early Precambrian metamorphic rock series, covered by Quaternary sediments up to 20 m thick (Fig. 1). The Mesozoic granites are mainly Jurassic Linglong granites, intruded by the Cretaceous Guojialing granodiorite, Weideshan

* Corresponding author. E-mail: mingchuns@163.com

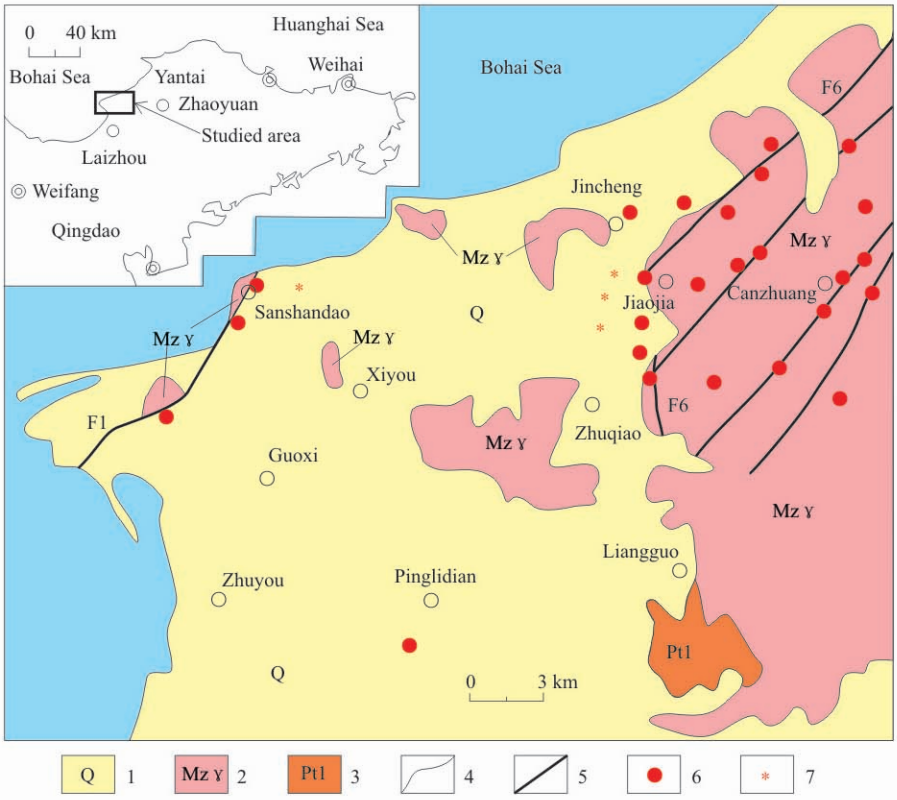

Fig. 1. Map showing geology and gold deposit distribution in the northwest part of Eastern Shandong Province.

1, Quaternary sediments; 2, Mesozoic granites; 3, Early Precambrian metamorphic rock series; 4, geological boundary; 5, fault; 6, position of shallow gold deposits (large ones with large diameters, and medium- to small-sized one with small diameter); 7, position of deep-seated gold deposits. F1, Sanshandao fault; F6, Jiaojia fault.

granites, Laoshan granites and some relevant dike rocks (such as lamprophyre, diabase-porphyrite, diorite–porphyrite and granitic dike). The Early Precambrian metamorphic rocks are mainly the late Archean Qixia gneiss suite and the Malianzhuang metagabbro, while a few occur in the Jiaodong rock group as residual inclusions. NE-trending faults are well developed, with the Sanshandao and Jiaojia faults as the main ones. Gold deposits occur in the fault structures, and large-scale gold deposits are distributed along the main faults, comprising the well-known Sanshandao and Jiaojia metallogenetic zones.

3 Gravitational and Magnetic Fields and Their Geologic Interpretation

3.1 Data and data processing

Based on a 1:25000 gravity survey and 1:10000, 1:5000 high-precision magnetic surveys, we have made magnetic and gravity maps covering an area of 500 km^2. Combined regional geological features with gold prospecting, the following methods for gravitational–magnetic data processing were adopted: (1) gridding process with grid distance as 100 m×100 m; (2) separating local gravity anomalies with different selected windows, obtaining regional gravity field and residual gravity anomalies, and making maps with 5 km×5 km windows; (3) upward continuations to heights of 500 m, 1000 m, 2000 m, 3000 m, 4000 m and 5000 m, respectively, to highlight deep geological bodies and reduce disturbance of shallow fields; (4) derivative value processing, horizontal first derivative process were done about an original plane data and different continuation heights in the direction of 0°, 45°, 90° and 135°, and vertical differential coefficients were done with the first and second derivate.

Four high-precision gravitational and magnetic profiles extending as long as 57 km were surveyed (profile location shown in Fig. 2), of which two profiles (No. II and IV) were also measured with magnetotelluric sounding (MT) and controlled source audio-frequency magnetotelluric method (CSAMT). Gravitational and magnetic data were processed with gridding and an upward and downward continuation with the grid distance of 100 m×100 m. We utilized the RGS2010 software developed by the China Geological Survey to do integrated inversion–simulation calculations of

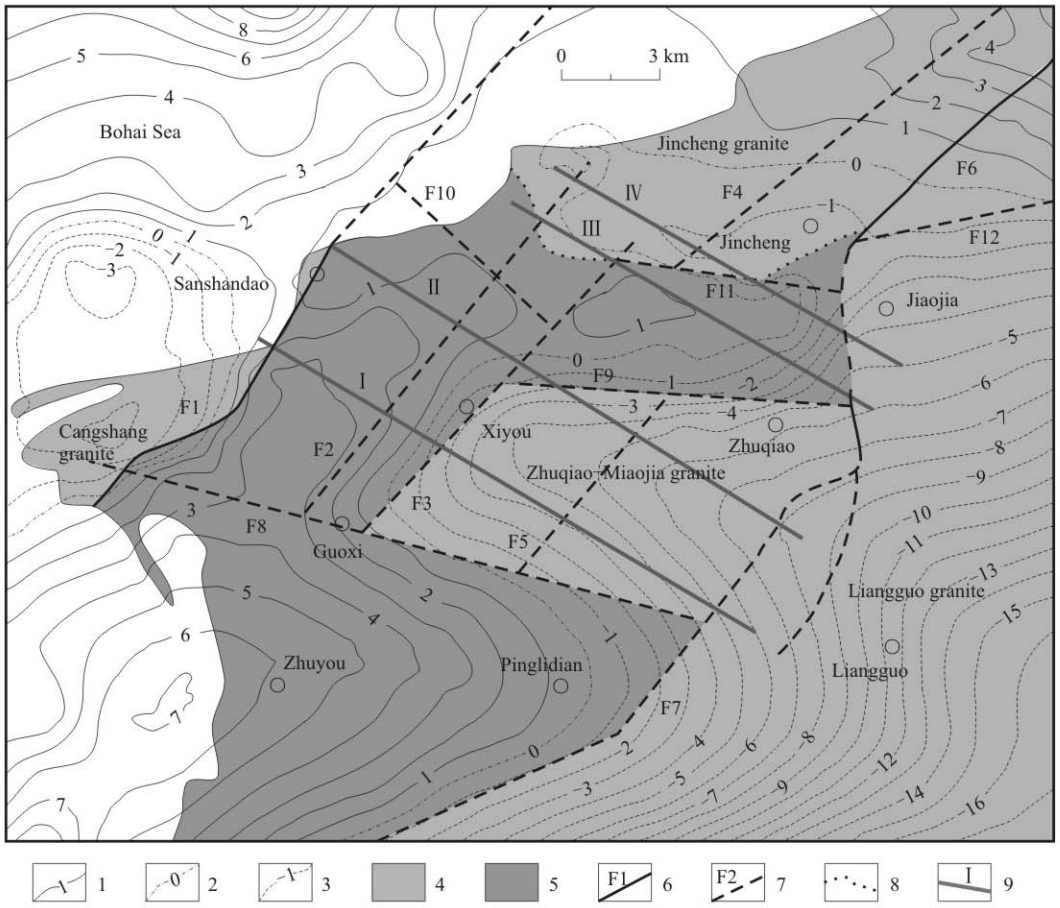

Fig. 2. Map showing bouguer gravity anomalies and gravitational-magnetic interpretation in the Sanshandao-Jiaojia area.
1, positive contours; 2, zero contours; 3, negative contours; 4, Mesozoic granites; 5, Early Precambrian metamorphic rock series; 6, measured faults; 7, inferred faults; 8, inferred geological boundary; 9, accurately measured gravitational–magnetic profile and number.

gravitational and high-precision magnetic data.

3.2 Gravitational and magnetic fields

Bounded by two NE-trending gravity anomaly belts, this study area forms a gravitational belt characterized by 'one high between two lows' (Fig. 2). The two gravity gradient zones are the Jiaojia and Sanshandao faults. The Sizhuang–Longbu section of the Jiaojia fault shows pronounced linear gradient anomalies whereas the south Sizhuang and north Longbu sections are in the torsional bending section of the bouguer anomaly contours. The east Jiaojia fault and the west Sanshandao fault are relatively low gravitational anomaly areas; between these two faults is a NWW-trending low between two highs. The gravitational field exhibits an increase from east to west, while from south to north it shows a characteristic 'three lows and three highs'.

The overall magnetic field shows NE-banded and moniliform characteristics, and that in the east Jiaojia fault and west Sanshandao fault is gentle, with the area between them chaotic (Fig. 3). The gentle magnetic field areas correspond to negative gravity anomalies; a chaotic one corresponds to positive gravity anomalies. A direct current (DC) composite profile suggests that the two ends are both high-resistivity anomaly areas, and in between is a low-resistivity anomaly area.

3.3 Interpretation of geological structures

3.3.1 Geophysical characteristics of main rocks

Metamorphic rocks in the study area are characterized by their high density and low–medium magnetism. These features are crucial to determining the positive gravity anomaly and jumped magnetic field. Magmatic rocks have high resistivity, low density and low magnetism. When the Mesozoic granites intruded the low-magnetism strata, a gentle positive magnetic anomaly was obtained, and then acidic rock bodies of some scale were able to form low-gravity anomaly areas. Large-scale fracture zones generally have low-density, low-magnetism, and can form low gravity, elongated, moniliform positive and negative magnetic anomaly areas. When they occur at the lithological contact zones, magnetic and gravitational

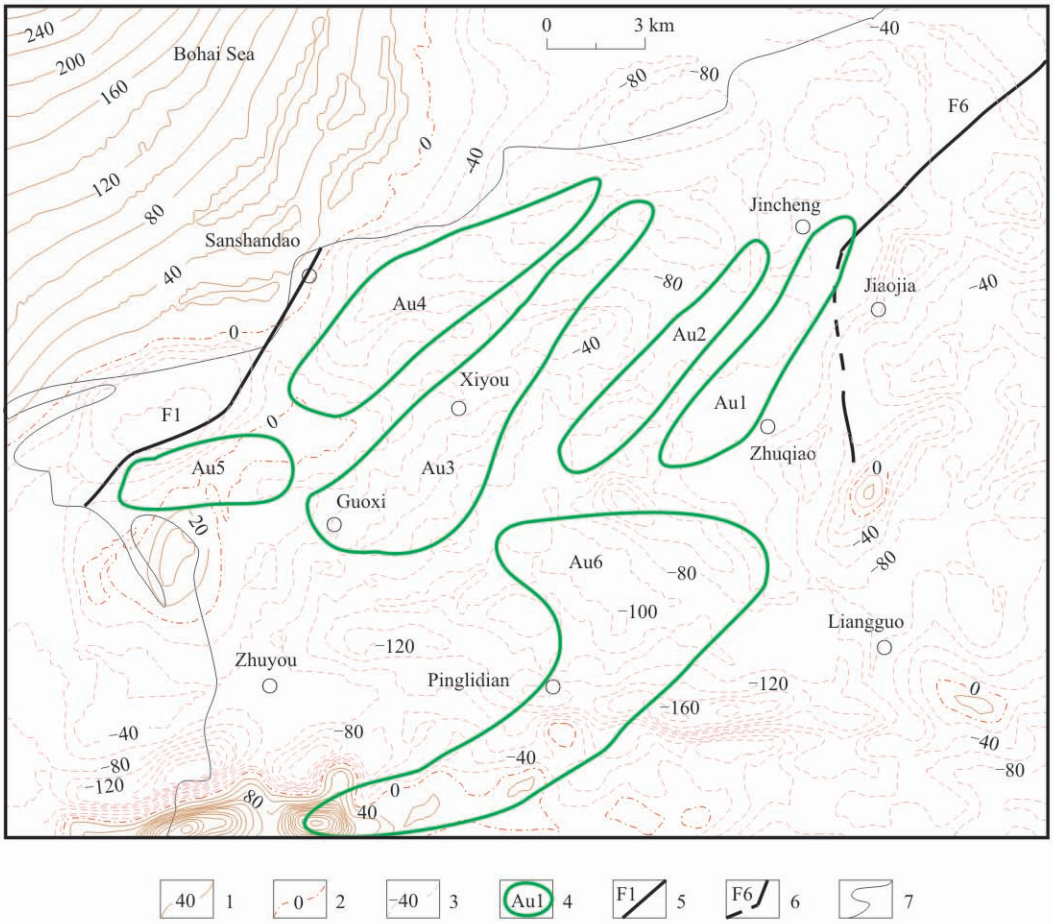

Fig. 3. Map showing anomaly curves $\triangle T$ and deep-seated gold targets.
1, positive contour; 2, zero contour; 3, negative contour; 4, deep-seated gold target and number; 5, Sanshandao Fault; 6, Jiaojia Fault; 7, coastline.

gradient belts are formed.

3.3.2 Interpretation of fault structures

Twelve faults were inferred overall in the region (Fig. 2), of which, seven NE-trending faults are intimately related with blocks and gold deposits, five NW-trending faults in the blocks are included; and five faults are consistent with the regional geology (F1–F5) and seven new inferred faults (F6–F12) are included. The faults F1 and F6 refer to the Sanshandao fault and Jiaojia fault, respectively.

Along the Sanshandao fault, the bouguer gravity anomaly yields a large-scale, large horizontal change rate gravity gradient zone. In the horizontal derivative (135°) anomaly map, the gradient exhibits as a long and narrow zone, and its horizontal change rate can reach 2.0×10^{-5}m/s^2/km. Integrated $\triangle T$ and the apparent resistivity anomaly show two different electric and magnetic field boundaries. In the western part, there is a gentle low negative magnetic field with a high-resistivity zigzag anomaly for apparent resistivity; whereas in the eastern part, there exists a chaotic magnetic field with a large variation from positive to negative values and a large horizontal change rate and a gentle low anomaly for apparent resistivity. Along the north section of the Sanshandao fault, the gravity gradient zone extends to the sea, while this fault is just in the contact zone between the gentle positive and negative magnetic fields. In magnetotelluric sounding profiles, the Sanshandao fault assumes a low-resistivity U-type anomaly. It is thus inferred that it is a large-scale deep fault that lies in the contact zone between the Early Precambrian metamorphic rocks and the Mesozoic Linglong granites at the shallow level, and intersects granitic bodies in the deep. This fault has an overall trend of 40°–50°, while the liner gravity–magnetism gradient zone assumes an S type in the plane, reflecting its varied trends. In the apparent resistivity profiles, this fault assumes low-resistivity U type. This may suggest that the fault dips to SE with a gentle wave shape, and that its dips become gentler downwards.

In the south Jiaojia fault (Longbu–Sizhuang section), the bouguer gravity anomaly, residual gravity anomaly and residual gravity difference anomaly together represent as significant gravity gradient zones. The vertical second

derivate anomaly of this fault is a long-extending zero contour and the horizontal derivative anomaly is a long and narrow zone, with a horizontal change rate of 3×10^{-5}m/s^2/km. The north section of the fault (to the north of Longbu) is developed in the Linglong granitic rock bodies due to the influence by the intersection of the nearly EW-trending rock bodies. On both sides of the fault there is no apparent density boundary. The gravity gradient zone has no significant reflection. The bouguer gravity anomaly represents the boundary between two different gravity fields, and the contours assume synchronous wiggle characteristics. Also, on both sides of the fault, the electric and magnetic fields show different characteristics. On the west side, the apparent resistivity curve assumes a gentle low-resistivity anomaly, with apparent resistivity between 200 to 300 Ω·m, while on the east side, it assumes a high-resistivity jumped anomaly, with apparent resistivity ranging from 500 to 1000Ω·m.

3.3.3 Interpretation of Early Precambrian metamorphic rock series

Based on gravitational, magnetic and electrical field characteristics, three types of distributing areas of the Early Precambrian metamorphic rock series are classified, i.e. metamorphic rock area, granitic rock area underlying the metamorphic rock and remnant metamorphic rock area in granites.

The metamorphic rock area is located in the Zhuyou–Pinglidian area, lying between faults F7 and F8 (Fig. 2). The bouguer gravity anomaly is shown as relatively high gravity, with a nearly EW-trending ellipse shape. The background value $\triangle$g is -3×10^{-5}m/s^2; the increased amplitude is 10.5×10^{-5}m/s^2; and the highest anomaly value is 7.5×10^{-5}m/s^2, reflecting the great rock thickness. In the $\triangle T$ anomaly map, it is expressed as an increased chaotic jumped positive/negative magnetic field area, ranging from −500 to 500 nT, with a northward decrease and a nearly EW-trending. The apparent resistivity is low, commonly lower than 200 Ω·m, with gentle anomaly contours. Quaternary sediments cover the whole area and metamorphic rock series is overlain by the Quaternary sediments (Zhang et al., 1989). With the increasing upward-continuation heights, the bouguer anomalies become stronger, and the zero boundaries gradually move westward. This may suggest that the metamorphic rock series have an 'thick in the east and thin in the west' distribution characteristic. Integrating the high-precision profile measurement with the bouguer gravity anomaly data, we infer that the thickness of the metamorphic rock near Zhuyou County is greater than 2500 m.

The granitic rock area underlying metamorphic rocks is located between the Sanshandao and Jiaojia faults. This area can be divided into two parts: (1) the first part is in the west of the study area, bounded by the faults F1, F3, F8 and F10 (Fig. 2). It is expressed as a NE-trending banded high anomaly, with a northward decreasing anomaly value. In the middle of this part, there is an open gentle gravity high, and at both ends there is a sharply decreasing gravity gradient zone, with a horizontal change rate of 2.5×10^{-5}m/s^2/km. Based on the magnetotelluric sounding profile, the first part can be divided into shallow (<−2000 m) low-resistance layer and deep (>−2000 m) high-resistivity layer. The resistivity exhibits an increase in ascending order, and at a depth of 2000 m, the variation gradient becomes significantly increased, forming a clear electric interface. In the integrated apparent resistivity profiles, the area is reflected as a southward-decreasing low-resistivity gentle anomaly. Its $\triangle T$ magnetic anomaly is expressed as a NE-trending striped relatively high magnetic anomaly, ranging from 0 to −40 nT, higher than the background value of the magnetic field in known granites (−60 nT). Through integrated gravitational–magnetic inversion calculations, the metamorphic rock thickness is known to be about 2000 m, with a 'thin on the east and west sides, thick in the middle' characteristic, where in the bottom and east and west sides are the Linglong granites. (2) the second part is bounded by the faults F3, F6, F9 and F11 (Fig. 2). The bouguer gravity anomaly exhibits an 'high in the west and low in the east' characteristic and decreases from middle to both south and north sides. In addition, the change rate of the gravity gradient zone in the southern part is significantly stronger than that in the northern part. As for the residual gravity anomaly, a local gravitational high covering an area of 2 km^2, west of the Matang area is developed in the eastern part, whereas that covering an area of 1 km^2 west of the Wujiazhuangzi area, reflects the localized thickening of the metamorphic rocks. In the $\triangle T$ magnetic anomaly maps, this part is expressed as an EW-trending moniliform relatively high magnetic anomaly. According to drilling work and positive and negative inversion calculations, the upper part is formed by the metamorphic rock series, while the lower part is the Linglong granite. In addition, the thickness of the metamorphic rocks gradually increases and near the western Wujiazhuangzi area, its thickness can reach as much as 2000 m.

The remnant metamorphic rock area in granites is distributed in the northeastern part of the study area, bounded by the faults F4, F6 and F11 (Fig. 2). It is reflected as a relatively high gravity area in the bouguer gravity anomaly and residual gravity anomaly maps. This anomaly is 4 km wide and extends northwesterly, with its peak value at 5.0×10^{-5}m/s^2. Gravity field characteristics suggest that this area exhibits a significantly higher

gravity anomaly than the Linglong granite, that is, an individual Linglong granite body cannot yield such a high gravity anomaly. The magnetic anomaly $\triangle T$ maps suggest that the magnetic field values show an eastward increase, significantly higher than that caused by granites. Its resistivity shows a jumped high-resistivity anomaly, consistent with the electrical characteristics of granites. It is thus inferred that the outcropping granites are overburden rock bodies, and the underlying metamorphic rocks exhibit an 'east thick and west thin' characteristic.

3.3.4 Interpretation of granites

Except for the above metamorphic rock distribution areas, other areas distribute the Linglong granites, which show clear negative gravity in the bouguer gravity maps and the residual gravity anomaly maps.

As shown in Fig. 2, the Cangshang rock body is located to the west of the Sanshandao fault. In the bouguer gravity and residual gravity anomaly maps, it has an ellipse shape with low gravity, and also with an elliptical magnetic field. These indicate that they share the same gravitational and magnetic source. The apparent resistivity characteristics show significantly high resistivity, differing from that on the east side of the Sanshandao fault where exist the low-resistivity gentle anomaly and elevated chaotic magnetic field. Exposure of sporadic granite bodies in the west Cangshang and Sanshandao area validates the existence of the granitic rock bodies.

The Liangguo rock body is located in the southeast of the study area, along the eastern side of the Jiaojia fault zone, and occupies the largest area in this region (Fig. 2). It shows significantly negative gravity in the bouguer and residual gravity anomaly maps. The gravity anomaly decreases from west to east, reflecting a gradual thickening of the rock bodies eastward. Its magnetic field is characterized by relatively gentle moniliform anomalies. The integrated apparent resistivity section is reflected as zigzag high-resistivity anomalies, and in the CSAMT sounding section, it is reflected as a high-resistivity basement.

The Zhuqiao–Miaojia rock body is lobe-shaped, protruding to the west, and is connected with the Liangguo rock body in the east, and is the westward part of the Liangguo rock body (Fig. 2). In the bouguer gravity anomaly and residual gravity anomaly maps, it is reflected as a nearly EW-trending lobe-shaped gravity low, and in the south and north sides and western ends, it is gravity high, forming significant ring-shape gravity gradient zone anomalies. This may indicate that the central part of the rock body rise high whereas the southern, northern and western flanks fall down greatly. Its magnetic field characteristics are NWW-trending banded relatively high anomalies, with a clustered surrounding magnetic field, which may suggest that on the upper part of the rock body there is a cover of relatively thin remnant metamorphic rocks.

The Jincheng rock body is located in the northern part of the study area, occurring as a NWW-trending lobe-shaped body protruding westwards. It is connected with the Liangguo rock body, and is part of the westward Liangguo rock body (Fig. 2). In the bouguer gravity anomaly and residual gravity anomaly maps, it is shown as a lobe-shaped gravity low. Its magnetic characteristics are relatively low gentle and clustered magnetic anomalies. The CSAMT sounding resistivity section is reflected as a shallow low-resistivity electric bed and a deep high-resistivity electric bed. Gravitational, magnetic and electrical field characteristics indicate that this rock body is a hidden one, the upper part of which is covered by some metamorphic rocks. The prospecting line No. 112 in the Jiaojia gold deposit suggests that the upper burial depth of this rock body is about 400 m (Cui, 2007), validating the existence of the hidden rock body.

Gravitational, magnetic and electrical field characteristics suggest that the metamorphic rocks between the Jiaojia and Sanshandao faults overlie in the Linglong granite, occurring as residual xenoliths. East of the Jiaojia fault zone and west of the Sanshandao fault, the Linglong granite outcrops, while between the Sanshandao and Jiaojia fault zones, the thickness of the metamorphic residual blocks are thin in the east and thick in the west, locally, the Linglong granite crops out due to erosion, with the erosional extents high in the east, low in the west, strong in the north, and weak in the south.

4 Geological–geophysical Metallogenic Model

4.1 Interpretation of integrated geophysical profiles

To study the extension variation of the main ore-controlling faults and to predict deep-seated gold deposits, four integrated geophysical profiles were surveyed in the Jiaojia and Sanshandao faults. Furthermore, integrated gravitational and magnetic inversion calculations and magnetotelluric (MT) sounding interpretation were carried out. Due to different lithology and geophysical properties, the fitting parameters were adopted as follows: for the Linglong granites, κ (magnetic susceptibility) $=246\times10^{-6}\times4\pi$SI, Mr (remnant magnetization) $=117\times10^{-3}$A/m, σ (density)$=2.58$g/cm^3; for metamorphic rocks, $\kappa=963\times10^{-6}\times4\pi$SI, $Mr=267\times10^{-3}$A/m, and $\sigma=2.81$g/cm^3; the density difference between the metamorphic rocks and the granites is 0.23 g/cm^3; the geomagnetic inclination is 54.761131°; the geomagnetism declination angle is －6.930224°; and the geomagnetic total field is

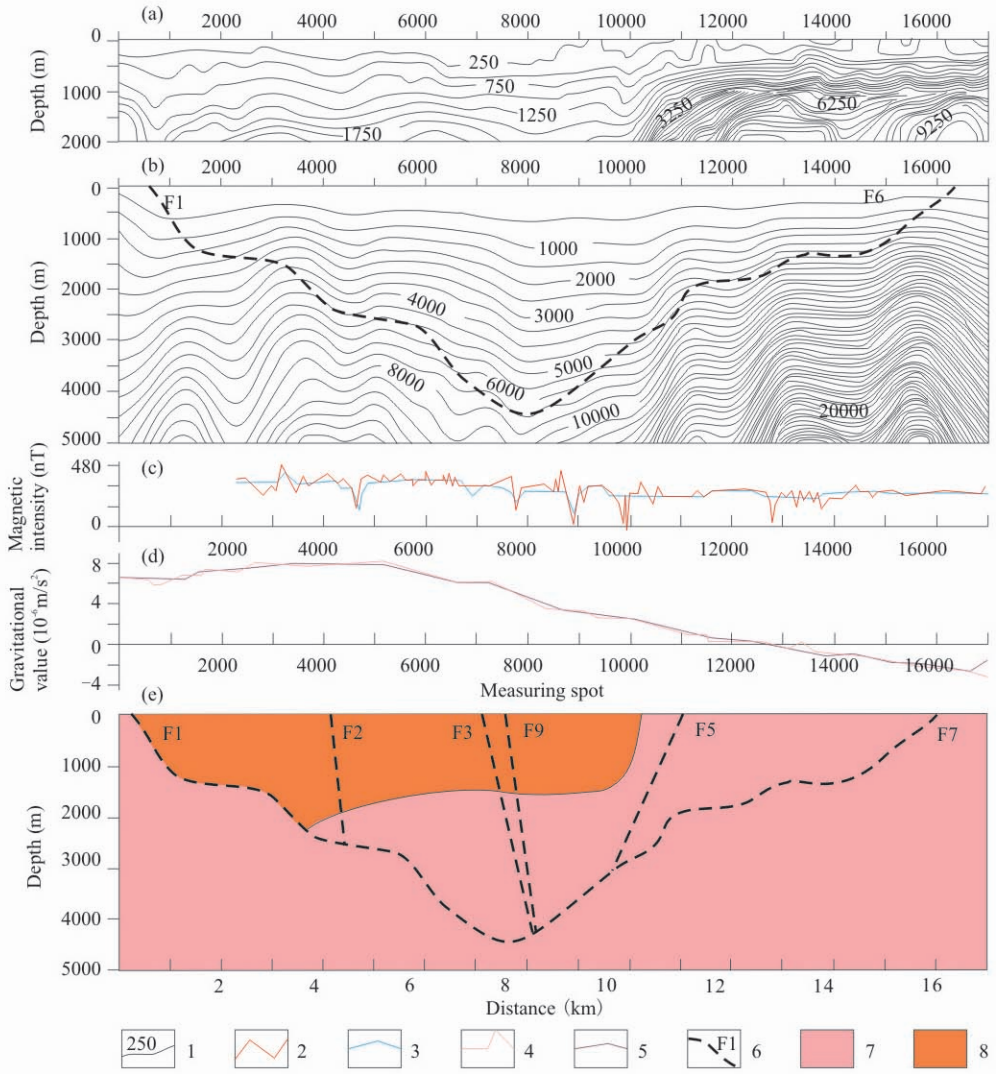

Fig. 4. Integrated inversion profile no. II based on gravity and magnetic data.
(a), CSMAT inversed apparent resistivity profile; (b), MT inversed apparent resistivity profile; (c), high-precision magnetic inversion profile; (d), gravity inversed profile; (e), inferred geological profile through inversion and calculation. 1, apparent resistivity contour; 2, measured geomagnetic anomaly (ΔT) curve; 3, theoretical geomagnetic anomaly curve; 4, measured gravity anomaly curve; 5, theoretical gravity anomaly curve; 6, inferred fault and number; 7, Mesozoic granite; 8, Early Precambrian metamorphic rock series.

52344 nT. The typical profile no. II was selected to do inverse modeling of the geological sections (Fig. 4).

According to its bouguer gravity anomaly features, profile no. II can be divided into three sections from west to east: (1) the western part from the Sanshandao fault (F1) to the Xiyou fault (F2), reflecting as high gravity, is in the metamorphic rock area; (2) the middle part from the Xiyou fault to the Zhaoxian fault is in the gravity gradient zone and in the contact zone between metamorphic rock and granites; (3) the eastern part (east of the F5 fault) is located in the Zhuqiao–Miaojia area, reflecting as low gravity. Inverse simulation (Figs. 4c, 4d) indicates that the metamorphic rock is distributed between the Sanshandao and Zhaoxian faults with a residual body. The metamorphic rock series to the east of the Zhaoxian area was eroded, and the Linglong granite is exposed. The thickness of the residual body of metamorphic rocks between the Sanshandao and Xiyou faults can reach as much as 1900 m, and the Linglong granite body underlies the metamorphic rocks (Fig. 4e). At depths shallower than 2000 m, the Sanshandao fault is near the contact zone between the Linglong granite body and metamorphic rock, whereas deeper than 2000 m it intersects with the Linglong granite. South section of the Jiaojia fault (F7) is in the granite body.

CSAMT sounding sections suggest that the electric characteristics shallower than 2000 m are jumped resistivity curves and clearly reflect the electric beds (Fig. 4a). Resistivity curves in the MT sounding sections are relatively smooth (Fig. 4b). This method is used to detect objects deeper than 2 km, with designed dot pitch as 300 m, and reflected depth as 5 km. Therefore, shallow electric

beds are not reflected clearer than those by the CSAMT method, but deep electric beds are reflected more clearly.

Based on the electrical characteristics (Figs. 4a, 4b), the section can be divided into three parts horizontally, i.e. high, medium and low resistivity anomaly areas. Areas between spots numbered from 11500 to 17000 in the east section are high apparent resistivity anomaly areas. Except for the shallow low-resistivity electric beds, resistivity is several ten of orders of magnitude higher than that in the west section, with dense resistivity contours and an increasing trend from top to bottom. This may suggest geophysical characteristics of granites. Areas between spots numbered from 5000 to 11500 in the middle of the section (F2–F5) are low resistivity anomaly areas, and are metamorphic rock area. Areas between spots numbered from 0 to 5000 (west of the fault F2) shows features between those above two areas. They show characteristics of 'high in the west and low in the east', an anomaly caused by the gradual uplift of the Linglong granite in the footwall of the Sanshandao fault.

Vertically, the section can be divided into upper low-resistivity and lower high-resistivity beds, and the resistivity exhibits gradually increasing features from top to bottom. There is a marked transitional gradient zones between the high-resistivity and low-resistivity beds. It is thus inferred the low-resistivity beds are Quaternary sediments and the metamorphic rock series whereas the high-resistivity beds are reflection of the Linglong granite.

The Sanshandao fault (F1) is a SE-dipping contact zone between high– and low– resistivity areas, the resistivity contours of which extend downward from west to east with a gentle wave form (Fig. 4b). Based on the different dips, the fault can be divided into three: (1) a section between spots numbered 200 to 2000, downward continuation of the height of which is around 2000 m, is the upper section of this fault. Resistivity curves bend downward, corresponding to the shallow steeply dipping part of the Sanshandao fault (dip about 60°); (2) the middle section is located between spots numbered from 2000 to 4500, with its depth between 2000 to 3000 m. The resistivity curves bend downward, with dips varying from steep to gentle. The above two sections lie in the contact zone between the metamorphic rock and granites; (3) the lower part is granites intersected by the Sanshandao fault, which is located between spots numbered 4500 to 7800, between faults F2 and F3, with downward continuation heights from 3000 to 4500 m. On the MT resistivity profile the bending angle of the resistivity contours increases significantly downward while the fluctuation of the resistivity curves is gentle. This may suggest that the fault varies from gentle to steep dipping, and that lithological and electrical properties between the hanging and foot walls have few difference. The areas with these anomaly features correspond to the bend transition zone of the curves. For areas between spots numbered 7500 and 9000, the resistivity curves are U-type, and with low resistivity characteristics; in the west part, the curve decreases on one side whereas in the east part, the curves gradually climb. Therefore, it is inferred that this is the intersection part between the Sanshandao and Jiaojia faults near the spot numbered 7500, and they intersect at a depth of about 4500 m.

The southern part of the Jiaojia fault (F7) trends west with a gentle wave shape from top to bottom, and intersects with the Sanshandao fault near the spot numbered 7500. In the CSMAT and MT resistivity section curve maps (Figs. 4a, 4b), there are westward and downward wave-like gradient zone anomalies. The fault can also be divided into 3 sections: (1) the upper part is between spots numbered from 14300 to 16000, with a downward continuation height of around 1200 m. The resistivity curves show a westward decrease and bending and thus it is inferred that the dip of this section is relatively steep. The low-resistivity gradient anomaly near the spot 16000 corresponds to the known surface structural alteration zone. (2) the middle part is between the spots from 11000 to 143000, equivalent to a depth from 1200 to 2000 m. In this part, the curves are gentle; the upper contour intervals of this part are wide whereas the lower contour lines are dense; a low-resistivity gradient zone in between dips gently downward with the dipping angles much smaller. (3) the lower part is between the spots from 11000 to 7500, with the curve dipping increasingly. Near spot No. 11000, the curves bend significantly. To the west of spot No. 10000, the curves tend to be gentler.

4.2 Geological-geophysical model for prospecting deep-seated gold deposits with the application of CSAMT and SIP methods

In order to establish geological–geophysical model for prospecting deep-seated gold deposits in the Jiaojia fault zone, integrated CSAMT and SIP (spectral induced polarization method) studies were done of the prospecting lines No. 264, 360 and 208 in the Sizhuang mine district, prospecting lines No. 128 and 112 in the Jiaojia mine as well as prospecting lines No. 135 and 143 in the Xincheng mine (Fig. 5). This model is responsible for the marked success in searching for deep-seated gold deposits in this region. The ore-controlling characteristics of the Jiaojia fault zone and the interpretation of the structures and gold bodies can be summarized as follows:

(1) Gold orebodies mainly occur in the footwall of the Jiaojia fault (Fig. 5d). In map view, the places where the

fault zone inflects, branching and re-merges are most favorable for mineralization. In profile, the places where the fault zone dilates and varies greatly in dip angles are most favorable for mineralization.

(2) In the CSAMT and MT apparent resistivity contour maps (Fig. 5a), the transitional gradient zone is the location of the fault zones. This is of a gentle wave shape, and the locations with maximal variation in gradient are the lower boundary of the main fault plane. The places where the apparent resistivity curves bend synchronously downwards, the contour interval increases and the occurrence changes from steep to gentle are the most favorable prospecting sites.

(3) In the SIP compound resistivity parameter section contour maps (Fig. 5b), the fault zone is reflected as a directional extension moniliform low-resistivity zone. The lower compound resistivity values indicate its strong mineralization extent. The sites of bending curves and localized enlargement of the low-resistivity zone are favorable for prospecting (Cao et al., 2009).

(4) In the charge rate parameter section curve maps (Fig. 5c), the fault zone is reflected as directional extension moniliform high-resistivity anomaly zones. Beyond some range, the higher the charge rate, the stronger the alteration and mineralization is.

(5) Gold orebodies are characterized by a high charge rate, a high time constant and low frequency.

4.3 Relationship between the Sanshandao fault and Jiaojia fault

The Jiaojia and Sanshandao faults are the major regional ore-controlling structures in this gold concentration area. These two faults have opposite inclination, with parallel strike and significantly similar characteristics. As for their geophysical characteristics, both of the fault zones are located in the gravity gradient zone, and their hanging walls are characterized by high gravity, a jumped magnetic field and low resistivity, while the footwalls are marked by low gravity, a relatively stable and gentle low magnetic field and high resistivity electric features. The faults are just in the contact zone between the high and low-resistivity areas.

The Jiaojia and Sanshandao faults share the following similar characteristics: (1) they both trends NE, with a parallel distribution. The shallow parts are distributed along the contact zone between the Linglong granite bodies and metamorphic rocks series whereas the deep parts intersect the granites; (2) they both extend gently with S shape in a plan view, and are characterized by steepness in the upper part and gentleness in the lower part, with listric fault features; (3) they both have a large-scale structural alteration zone and main successive and stable fault planes. Below the main fault planes, there developed a 10–50 cm thick gray fault gouge, and further below there are cataclasite, granitic cataclasite and fractured granite, or beresite(pyrite-phyllic-alteration rock), beresitized granitic cataclasite and beresitized granite; (4) both faults are gold-controlling structures. The main fault zones develop the Jiaojia-type altered gold deposits, and below this there are stockwork-gold and lode-gold mineralizations; (5) fault activity characteristics and sequences are concordant, i.e. in the early stage there was ductile deformation, which was followed by brittle fault activities, including tenso-shear activity in the main mineralization stage and compressor-shear activity later (Miao et al., 1997; Li et al., 2002; Wang et al., 2003; Li et al., 2005).

Similarities between the Jiaojia and Sanshandao faults suggest that they were both formed under the same tectonic background and tectonic regime. We consider that these two faults and the Zhaoping fault together comprise a large-scale extensional structural zone along the boundary of the Linglong granites and Early Precambrian geological bodies (Song et al, 2008). Based on the above geophysical data, coupled with the geological and mineral exploration data, we infer that the Jiaojia and Sanshandao faults intersect at depth along the Guoxi–Xiyou–Wujiazhuangzi–Yuanjia area, with their intersection depth 4500 m below the surface. The hanging wall between the Sanshandao and Jiaojia faults is mainly Early Precambrian metamorphic rocks; the shallow parts of the faults run along the contact zone between the metamorphic rock and the granites, and the deep parts intersect the Linglong granite. On the footwall of the fault occurs exclusively Linglong granite. These two faults exhibits listric fault nature overall, steep in the upper parts and gentle in the lower parts, extending along the dip with smooth undulation. From the surface to the intersection of the faults, they have several sections with their dip angle varying a lot, forming step distribution along the inclination. Deep-seated gold orebodies occur on the steps with changing dip angles; the Jiaojia and Sanshandao faults each have two steps with clear change of inclination in their deep parts, correspondingly forming four predicted targets (Fig. 6).

5 Deep-Seated Gold Prospecting Targets

5.1 Jincheng–Qianchenjia target (Au 1)

This target is located in the Jincheng–Zhuqiao area belonging to the hanging wall of the Jiaojia fault, and is covered by Quaternary accumulations (Fig. 3). It is located in the second step extending along inclination of the Jiaojia fault, with varied dips. Above the second step, there is the

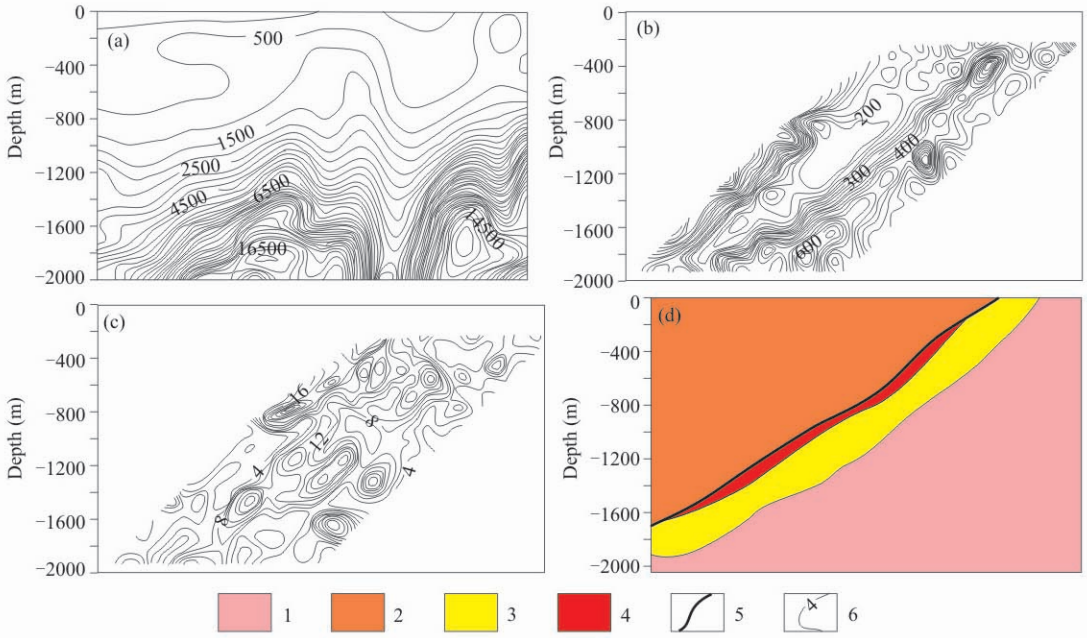

Fig. 5. Geological–geophysical prospecting model for deep-seated gold deposit prospecting.
(a), CSMAT apparent resistivity section; (b), SIP complex resistivity section; (c), SIP charging rate section; (d), geological profile. 1, Jurassic Linglong granite; 2, Early Precambrian metamorphic rock series; 3, structural alteration zone; 4, gold orebody; 5, fault structure; 6, contour and value.

first step where the dip angle of the fault changes from steep to gentle, and this is the shallow gold mineralization area or the first mineralization zone. The Jincheng–Qianchenjia target area is then just in the deep second mineralization zone (Fig. 6).

This area is in the transition area, with a contour gradient belt changing from gentle to steep in the CSAMT and MT resistivity maps. The upper parts are relatively low-resistivity electrical beds whereas the lower parts are relatively high-resistivity electrical beds. In the gravity anomaly maps, it is in the transition zone of the gravity gradient zone, and in the middle are nearly EW-trending nose-type high-gravity values. The magnetic field characteristics indicate local closed high magnetic anomalies in the negative magnetic background. Interpretation of integrated gravitational, magnetic and electric profiles suggests that the dip angle of the main fault plane of the Jiaojia fault varies considerably in the target area, and areas between spots numbered 7800 to 8000 in profile IV and areas between spots numbered from 8000 to 9000 in profile III are the favorable deep prospecting areas.

5.2 Xiaoxizhuang–Zhaoxian target (Au 2)

This target is located between the Bunanyinjia and Xiaoxizhuang areas in the middle part of the study area, in

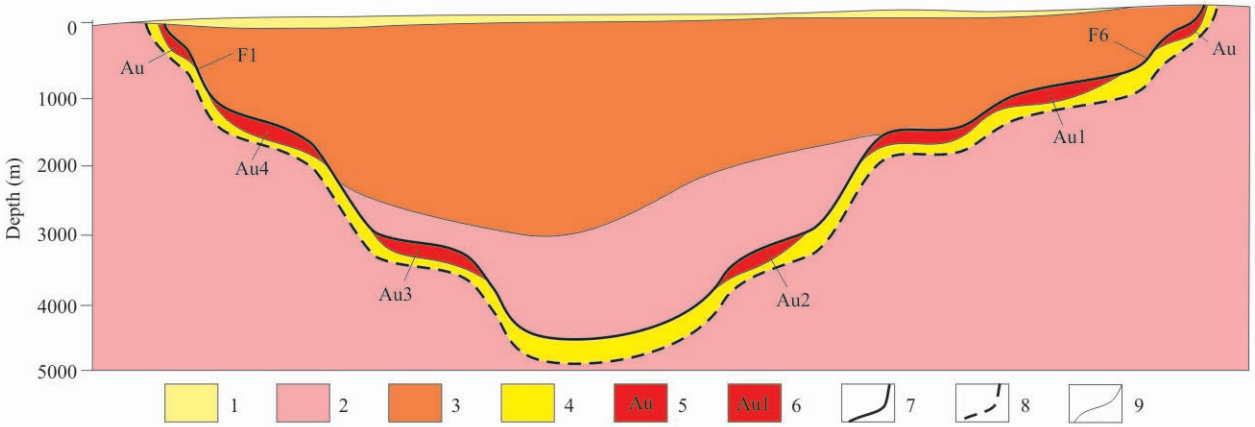

Fig. 6. Relationship between the Jiaojia and Sanshandao faults and deep prospecting prediction.
1, Quaternary sediments; 2, Mesozoic granites; 3, Early Precambrian metamorphic rock series; 4, mineralized alteration zone; 5, shallow gold orebody; 6, deep-seated gold prospecting target and number; 7, fault structure; 8, alteration zone boundary; 9, geological boundary. F1, Sanshandao Fault; F6, Jiaojia Fault.

the contact zone between the metamorphic rock series and the Linglong granite. The Linglong granites outcrop in the southwestern part of this area, which is controlled by the Jiaojia Fault (Fig. 3). In gravity anomaly maps, this is nearly EW-trending nose-type gravity high. In the southern and northern ends, it is expressed as a lobe-shaped gravity low protruding westward, whereas in the middle the contours exhibit an inward sag appearance. The magnetic anomaly is shown as moniliform banded form. In the CSAMT and MT resistivity profiles, the target is in the transition zone of the contour gradient zone that varies from gentle to steep. Its upper parts are relatively low resistivity electric beds whereas the lower parts are relatively high resistivity electric beds. Gravitational and magnetic data indicate its southern parts are the Linglong granites, in the middle are the metamorphic rocks, while the northern parts are hidden Linglong granites. Integrated profiles suggest that the target is in the third step, which extends along the inclination of the Jiaojia fault with smoothly undulating shape; it is located in the deep third mineralization zone (Fig. 6). Areas between spots numbered from 6000 to 7000 in profile IV and areas between spots numbered from 6000 to 7500 in profile III are the most favorable areas for deep prospecting.

5.3 Xiyou–Wujiazhuangzi target (Au 3)

This target termed Au 3 is located in the Xiyou–Wujiazhuangzi area where the Sanshandao fault exerts critical control and the bedrock is covered by Quaternary sediments (Fig. 3). Gravity anomalies are positive in the west and negative in the east, while the predicted area is just in the transition zone of the gravity anomaly gradient zone. The magnetic field shows as a banded high anomaly in the negative magnetic background. In the MT profiles, the target is at the bottom of the low-resistivity U-type anomaly. Integrated studies show this target is located in the third step of the Sanshandao Fault with varied dip angle for the main fault plane and an extended area along inclination; it belongs to the third mineralization zone (Fig. 6).

5.4 Xiangyangling–Xinlicun target (Au 4)

Located in the Cangshang–Xiangyangling–Xinlicun area, the target Au 4 is also controlled by the Sanshandao fault zone and covered by Quaternary sediments at the surface (Fig. 3). This target area is in the NE-trending high gravitational anomaly area, the western part of which is a linear gravitational gradient zone. The magnetic field is shown as high-banded magnetic anomalies. There are mainly metamorphic rocks, and in the western part there are contact zones between the metamorphic rocks and the granites. In the CSAMT and MT resistivity profiles, the contour gradient zone is reflected as a gentle to steep transitional zone. In the upper part, it is a relatively low resistivity electrical bed, while in the lower part it is relatively high resistivity electrical bed. Comprehensive studies of the profiles show that this target area is located in the second step that extends along inclination of the Sanshandao fault with a smooth undulating shape and a marked change in dip angle of main fault plane, and belongs to the second deep mineralization zone (Fig. 6). Above it is the first step along the Sanshandao fault the dip angle of the fault changes from steep to gentle, and is the known shallow gold concentration area and called as the first mineralization zone. Areas between spots numbered from 1500 to 3000 in profile I and spots numbered between 3000 and 4000 in profile II are the most favorable metallogenic areas.

5.5 Panjiawuzi target (Au 5)

This target Au 5 is located in the Cangshang–Panjiawuzi area southwest of the study area, the surface of which is covered by Quaternary sediments (Fig. 3). Gravitational and magnetic anomaly characteristics are shown as a large-scale liner gradient zone, belonging to part of the Cangshang anomaly area. In its western part, there are gravitational and magnetic lows, whereas the east has gravitational and magnetic highs and thus it is inferred that Au 5 is the contact zone between the metamorphic rock and the granites. West of the contact zone are low gravitational and magnetic granite areas, whereas in the east are high gravitational and magnetic metamorphic rock areas.

5.6 Miaojia–Pinglidian target (Au 6)

Au 6 is located in the southern extended part of the Jiaojia fault zone. This target is distributed along the Ziluoliujia–Miaojia–Caojiabu-Junzhaizhi area, most of which is covered by Quaternary sediments (Fig. 3). Gravitational and magnetic anomalies are characterized by a large-scale gravitational–magnetic linear gradient zone. To the east of this zone is an large area with low gravity and low magnetic force; to the west is an area with high gravitational and magnetic anomalies; to the north there is a EW-trending gravity low protruding to the west and in a torsional bending section of the gravitational anomaly contours whereas the south part is just in the gravitational linear gradient zone. It is thus inferred that the north part is in the granite bodies, while the south is in the contact zone between metamorphic rock and granites. Significant geophysical anomaly characteristics indicate large-scale hidden fault structures favoring metallogenesis in this region.

Targets Au 1 to Au 4 are distributed along the steps of

the Jiaojia and Sanshandao faults, where the dip angles of the faults vary from steep to gentle along their inclination, forming step-like distribution pattern of orebodies in space. This may validate a step metallogenic model in the northwest Jiaodong peninsula (Song et al., 2012). This model can be summarized as follows: fault structures exert a key control on gold metallogeny in the northwest Jiaodong peninsula; three ore-controlling faults, i.e. the Sanshandao, the Jiaojia and the Zhaoping faults, are actually in the same large-scale extensional fault zone; gold deposits occur in the footwall of the fault structures; the Jiaojia-type gold deposits occur near the main fault plane, while the Linglong-type gold deposits are a little farther from the main fault plane; the faults are distributed with a listric form in profile. These faults form several steps, of which the dip angles vary from steep to gentle with increasing depth. Correspondingly, several deep mineralization spaces are thus formed; the thicker parts of the gold bodies occur in the gentle parts, which form the characteristic step-type distribution. In the Cretaceous, mantle uplift, lithospheric thinning in eastern China caused strong tectonic-magmatic activities which are the dominant factor of gold mineralization in eastern Shandong(Liu et al., 2001; Zai et al., 2001; Zhou et al., 2002; Chen et al., 2004; Deng et al., 2004; Mao et al., 2005; Dong et al., 2008; Wan and Zhu, 2011).

6 Conclusions

The gravity field in the Sanshandao–Jiaojia area is bounded by two NE-trending gravity gradient zones, i.e. the Jiaojia fault zone and the Sanshandao fault zone, forming a 'one high between two lows' anomaly area. The magnetic fields are NE-trending striped and moniliform chaotic ones, which are gentle in the eastern and western parts, whereas chaotic in the middle part. Twelve faults are inferred overall, of which seven NE-trending faults are intimately associated with blocks and gold metallogeny, whereas five NW– and EW-trending faults are developed in the blocks. Areas east of the Jiaojia fault and west of the Sanshandao fault exhibit geophysical characteristics of the Linglong granites. Areas between the Jiaojia fault zone and the Sanshandao fault zone are remnant metamorphic rock, with eastward-thinning remaining thickness. They include metamorphic rock area, granitic rock area underlying the metamorphic rock and remnant metamorphic rock area in the granites. The Linglong granite distribution area can be divided into four rock bodies of granite with a little difference in geophysical characteristis, i.e. the Cangshang, Liangguo, Zhuqiao-Miaojia and Jincheng. The resistivity contours along the Sanshandao and Jiaojia faults extend gently, and these two faults intersect at a depth of 4500 m. These two faults extend along their inclination, and the faults each have two steps with significantly changing dips, becoming the gold target areas at depth that has a step-like distribution pattern. The six predicted deep-prospecting target areas are the Jincheng–Qianchenjia, Xiaoxizhuang–Zhaoxian, Xiyou–Wujiazhuangzi, Xiangyangling–Xinlicun, Panjiawuzi and Miaojia–Pinglidian target areas.

Acknowledgements

This work is granted by the Geological Science and technology foundation of Shandong Provincial Bureau of Geology and Mineral Resources (Grant No. 20080037). We thank Mr. Jiang Hongli and Cui Shuxue from No.6 Exploration Institute of Geology and Mineral Resources of Shandong Province for their help in the field work. Thanks to Professor Haoziguo of the Geological Society of China for kind help.

Manuscript received Mar. 2, 2012
accepted Mar. 28, 2012
edited by Susan Turner

References

Cao Chunguo, Feng Guoyan and Liu Hong, 2009. Theory and application of SIP technology in metal exploration in deep. *Land and Resources in Shandong Province*, 25(9): 42–46 (in Chinese with English abstract).

Chen Yanjing, Pirajno Franco, Lai Yong and Li Chao, 2004. Metallogenic time and tectonic setting of Jiaodong gold province, eastern China. *Acta Petrologica Sinica*, 20(4): 907–922 (in Chinese with English abstract).

Cui Shuxue. 2007. Analysis on south extending and ore prospecting future of Jiaojia fault belt. *Land and Resources in Shandong Province*, 23(10): 7–10 (in Chinese with English abstract).

Deng Jun, Wang Qingfei, Yang Liqiang, Wang Jianping, Gao Bangfei and Liu Yan, 2004. The geological settings to the gold metallogeny in northwestern Jiaodong Peninsula, Shandong Province. *Earth Science Frontiers* (China University of Geosciences, Beijing), 11(4): 527–533 (in Chinese with English abstract).

Dong Shuwen, Zhang yueqiao, Long Changxing, Yang Zhenyu, Ji Qiang, WangTao, Hu Jianming and Chen Xuanhua, 2008. Jurassic tectonic revolution in China and new interpretation of the "Yanshan movement". *Acta Geologica Sinica* (English edition), 82(2): 334–347.

Gu Liucheng, Wan Guopu and Duan Linxiang, 1996. *Geological-geophysical-geochemical modes of the fracture zone-hosted alteration rock gold deposits in the eastern Shandong Province and their evaluation indicators*. In: Shandong Provincial Bureau of Geology & Mineral Resources, Shandong Geology and Minerals Work. Jinan: Shandong Science and Technology Press, 178–193 (in Chinese).

He Hao, Meng Qingmin, Man Tinglong and Gao Weidong,

2005. The application of airborne geophysical (electric, magnetic) integrated survey to gold exploration in Jiaodong area. *Geophysical and Geochemical Exploration*, 29(5): 397–400 (in Chinese with English abstract).

Jiang Weiwei, Hao Tianyao and Yu Changming, 1997. The study of comprehensive geology and geophysics of Bailidian, Qixia, Shandong. *Process in Geophysics*, 12(2): 41–49 (in Chinese with English abstract).

Li Houmin, Shen Yuanchao and Liu Tiebing, 2002. Genetic relationship between Jiaojia-type and Linglong-type gold deposits in northwestern Jiaodong district, Shandong Province. *Mineral Deposits*, 21(Suppl.): 621–624 (in Chinese).

Li Junjian, Luo Zhenkuan, Liu Xiaoyang, Xu Weidong and Luo Hui, 2005. Geodynamic setting for formation of large-superlarge gold deposits and Mesozoic granites in Jiaodong area. *Mineral Deposits*, 24(4): 361–372 (in Chinese with English abstract).

Li Shixian, Liu Changchun, An Yuhong, Wang Weicong, Huang Tailing and Yang Chenghai, 2007. *Geology of gold deposits in Jiaodong*. Beijing: Geological Publishing House, 122, 280–294 (in Chinese).

Liu Jianming, Ye Jie, Xu Jiuhua, Jiang Neng and Ying Hanlong, 2001. Preliminary discussion on geodynamic background of Mesozoic gold metallogeny in eastern north China—with examples from eastern Shandong Province. *Progress in Geophysics*, 16(1): 39–46 (in Chinese with English abstract).

Mao Jingwen, Li Houmin, Wang Yitian, Zhang Changqin and Wang Ruiting, 2005. The relationship between mantle-derived fluid and gold ore-formation in the eastern Shandong Peninsula: evidences from D-O-C-S isotopes. *Acta Geologica Sinica*, 79(6): 839–857 (in Chinese with English abstract).

Miao Laicheng, Luo Zhenkuan, Guan Kang and Huang Jiazhan, 1997. The evolution of the ore-controlling faults in the Zhaoye gold belt, Eastern Shandong Province. *Contributions to Geology and Mineral Resources Research*, 12(1): 26–35 (in Chinese with English abstract).

Niu Rubao and Luowei, 1995. Study on the comprehensive information of geophysics and its application in gold prospecting in the Jiaojia gold field, Shandong Province. *Geology in Shandong*, 11(1): 68–76 (in Chinese with English abstract).

Niu Rubao, Wang Lunji, Wang Youfang, Song Haiping, Pang Xugui, Zhao Xiantang and Han Yanli. 2004. Application of resistivity depth sounding to the deep alteration zone of the Jiaojia type gold deposit. *Mineral Resources and Geology*, 18 (1): 69–72 (in Chinese with English abstract).

Song Mingchun, Meng Qingbao, Yang Chenghai, Jiao Xiumei, Cui Shuxue, Yang Zhili and Jiang Hongli, 2007. Discovery of the super-large deep gold deposits in the Sizhuang ore district, Shandong Province and its metallogenic significance. *Geology in China*, 34(Suppl.): 220–224 (in Chinese with English abstract).

Song Mingchun, Cui Shuxue, Yang Zhili, Jiang Hongli, Yang Chenghai and Jiao Xiumei. 2008. Great progress and far-reaching significance of deep exploration in the Jiaojia metallogenic belt, Shandong Province. *Geology and Exploration*, 44(1): 1–8 (in Chinese with English abstract).

Song Mingchun, Cui Shuxue, Zhou Mingling, Jiang Hongli, Yuan Wenhua, Wei Xufeng and Lü Guxian, 2010a. The deep oversize gold deposit in the Jiaojia field, Shandong Province and its enlightenment for the Jiaojia-type gold deposits. *Acta Geologica Sinica*, 84(9): 1349–1358 (in Chinese with English abstract).

Song Mingchun, Cui Shuxue, Yi Pihou, Xu Junxiang, Yuan Wenhua and Jiang Hongli, 2010b. *Prospecting and metallogenic model of the large and super-large deep-seated gold deposits in the gold concentration area, Northwest Jiaodong Peninsula, Shandong Province*. Beijing: Geological Publishing House, 57–108 (in Chinese).

Song Mingchun, Yi Pihou, Xu Junxiang, Cui Shuxue, Shen Kun, Jiang Hongli,Yuan Wenhua and Wang Huajiang, 2012. A step metallogenetic model for gold deposits in the northwestern Shandong Peninsula, China. *Science China Earth Sciences*, 55 (6): 940–948.

Wan Tianfeng and Zhu Hong, 2011. Chinese continental blocks in global paleocontinental reconstruction during Paleozoic and Mesozoic. *Acta Geologica Sinica* (English edition), 85(3): 581–597.

Wang Jincao, Xia Bin and Tang Jingru, 2003. Recognition on some key geological problems of Linglong-Jiaojia ore concentrated district in Shandong province. *Geotectonica et Metallogenia*, 27(2): 147–151 (in Chinese with English abstract).

Yang Jinzhong, Zhao Yuling, Shen Yuanchao and Shi Kunfa, 2000. Application research of controlled source acoustic magnetotelluric in the location forecasting of buried orebodies. *Geological Science and Technology Information*, 19(3): 107–112 (in Chinese with English abstract).

Zhang Huaquan, Shi Yongfa and Liu Guangzhi, 1989. The evaluation of metallogenic prospect of Pinglidian gold mining area in Laizhou, Shandong Province. *Gold Geology*, 4(4):33–37 (in Chinese with English abstract).

Zhou Ming, 1989. The effectiveness of magnetic survey in eastern Shandong gold ore belt. *Geophysical and Geochemical Exploration*, 13(4): 266–272 (in Chinese with English abstract).

Zhai Mingguo, Yang Jinhui and Liu Wenjun, 2001. Large clusters of gold deposits and large-scale metallogenesis in Shandong Peninsula, eastern China. *Science in China* (series D), 31(7): 545–552 (in Chinese).

Zhou Xinhua, Yang Jinhui and Zhang Lianchang, 2002. The formation of the ultra-large gold deposits in Shandong Peninsula in relation to deep processes of lithosphere in North China Craton. *Science in China* (series D), 32(Suppl.): 11–20 (in Chinese).